Global distribution of atmospheric waves in the equatorial upper troposphere and lower stratosphere: AGCM simulation of sources and propagation

Yoshio Kawatani[1], Masaaki Takahashi[1,2], Kaoru Sato[3]
Simon Alexander[4,5], Toshitaka Tsuda[5]

1. FRCGC/JAMSTEC, 2. CCSR Univ. Tokyo, 3. Univ. Tokyo
4. Australian Antarctic Division, 5. RISH Kyoto Univ.

<abstract>

- The global distribution, sources, and propagation of atmospheric waves in the equatorial UTLS region were investigated using an AGCM
- QBO-like oscillation with a period of ~1.5-2 years was simulated well without gravity wave drag parameterization
- The AGCM simulated realistic convectively coupled equatorial trapped waves (EQWs) and EQWs in the stratosphere.
- EQWs with 8<h<90 m from the n = -1 to n = 2 mode were extracted.
- Each EQW in the stratosphere generally corresponded well with the source of each convectively coupled EQW activity in the troposphere.
- Distributions of stratospheric PE due to EQWs are affected by (1) source distribution, (2) Walker circulation, and (3) the QBO phase
- EQWs with vertical wavelengths≤7 km contribute up to ~30% of total potential energy≤7 km over the equator at an altitude of 20-30km.
- Gravity waves generated by cumulus convection with period ≤ 24 h are clearly visible over areas of Africa and the Amazon etc, which result in localized PE in areas short distances from the source region.
- Comparisons of the AGCM results and COSMIC GPS RO results

EH: eastern hemisphere
WH: western 〃
PE: potential energy
EQW: equatorial trapped wave
Uz>0: westerly shear of the zonal wind
Uz<0: easterly shear 〃
Cx: horizontal phase velocity relative to ground

<Model description>

CCSR/NIES/FRCGC AGCM ver. 5.6 (K-1 Model developers 2004)
T106L60 (⊿h=120km, ⊿z=550m in the UTLS) with top at ~50km
No gravity wave drag parameterization
Realistic topography and climatological SSTs
Arakawa-Schubert (1974) type cumulus parameterization
Relative humidity limit method incorporated (Emori et al. 2001)
3-hourly output for 4 analyzed periods (see below figure)

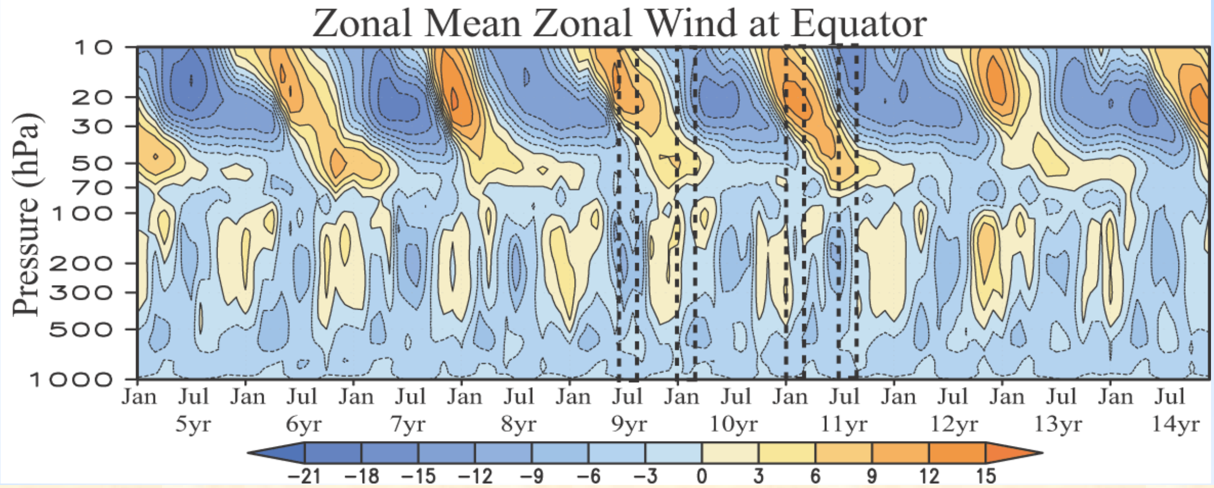

QBO-like oscillation

period: ~1.5-2yr

Fig.1: Time-height cross-section of zonal-mean U at the equator. Boxed areas with dashed lines indicate the periods analyzed

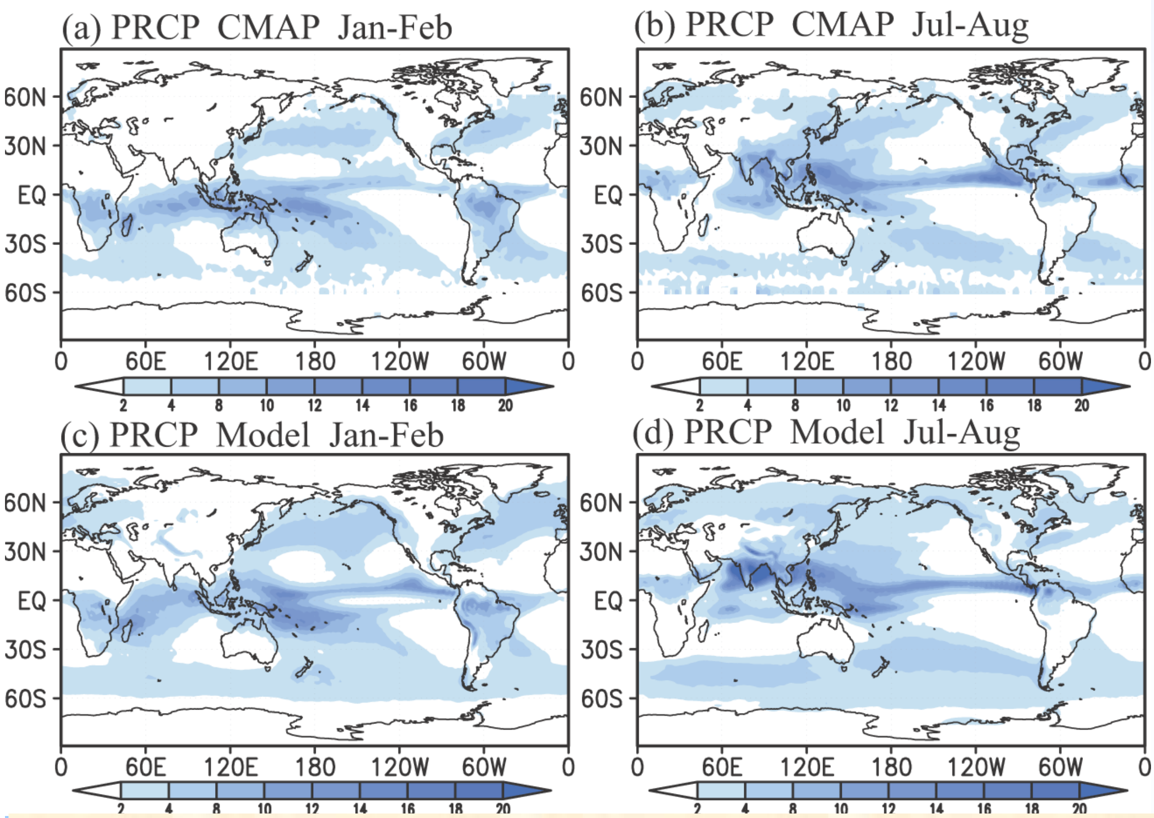

well simulate rainfall area

ITCZ

SPCZ

Indian monsoon

Africa

South America

Fig.2: Precipitation (mm day^{-1}) in (a, c) Jan-Feb and (b, d) Jul-Aug (a, b) CMAP (23-years mean) and (c, d) the model (17-years mean)

Evaluate how well the model simulates convectively coupled EQWs: Space-time spectral analysis of precipitation according to the method of Lin *et al.* (2006) using daily data from the GPCP and the model output

Grid data D(ϕ) as a function of latitude ϕ expressed as the sum of symmetric DS(ϕ) and antisymmetric DA(ϕ)

$$D(\phi) = DS(\phi) + DA(\phi)$$
$$DS(\phi) = \left[D(\phi) + D(-\phi)\right]/2$$
$$DA(\phi) = \left[D(\phi) - D(-\phi)\right]/2$$

The dispersion relation of EQW modes in shallow-water equations on an equatorial beta plane (Matsuno 1966)

$$\frac{\hat{\omega}^2}{gh_e} - k^2 - \frac{k\beta}{\hat{\omega}} = (2n+1)\frac{\beta}{\sqrt{gh_e}} \quad for\ n = 0,1,2..., \qquad \hat{\omega} = -Nk\left[\frac{N^2}{gh_e} - \frac{1}{4H^2}\right]^{-1} \quad for\ Kelvin\ wave\,(n=-1)$$

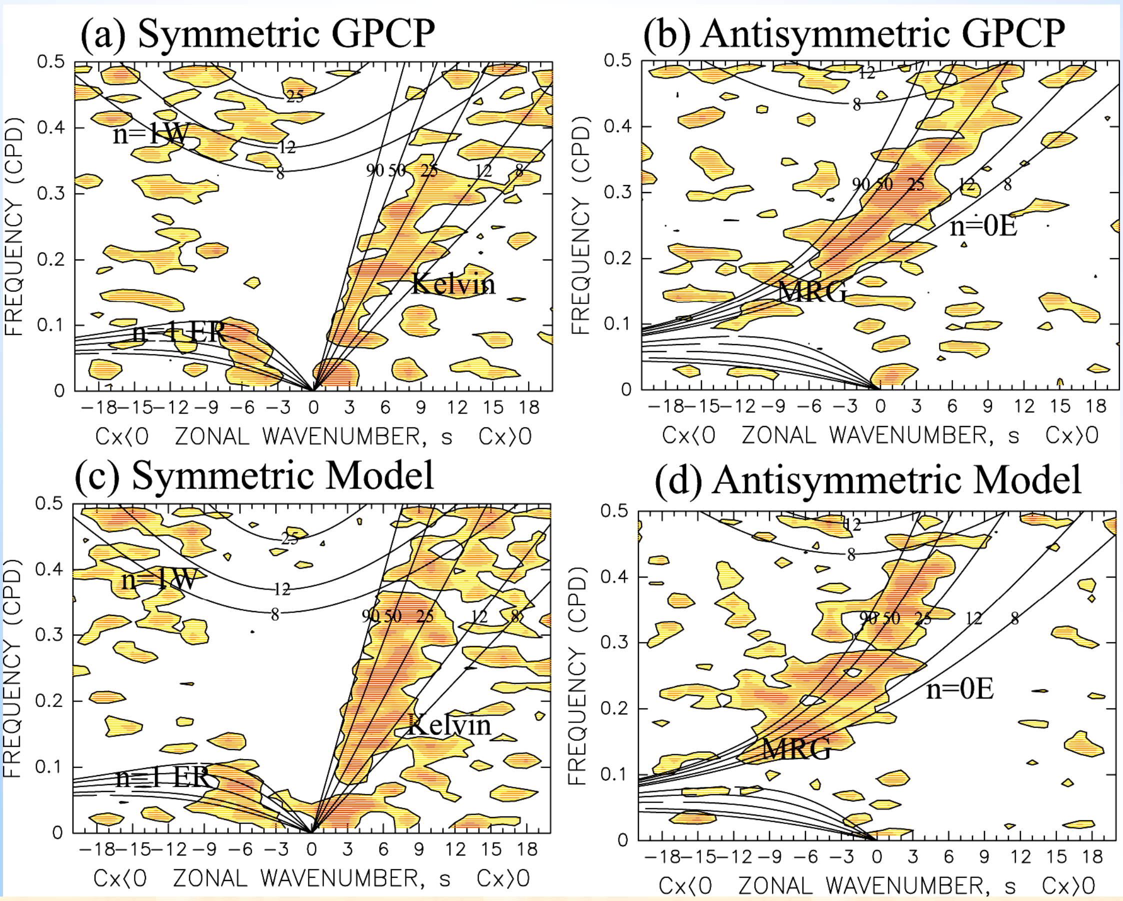

Symmetric n= -1 & 1

Antisymmetric n= 0 & 2

equivalent depths *he:* 8, 12, 25, 50, 90 m

$$\lambda z = 2\pi\left[\frac{N^2}{gh_e} - \frac{1}{4H^2}\right]^{-1/2}$$

Fig.3: Zonal wavenumber *vs.* frequency spectra of precipitation divided by the background spectra (15N-15S average); values ≥ 1.1 are shown (a, c) Symmetric and (b, d) antisymmetric components of precipitation (a, b) Observation and (c, d) model. Frequency spectral width: 1/128 cpd

- The wave spectrum in the middle atmosphere is linked to the variability of convective precipitation (Horinouchi et al. 2003)
- **The well simulated spectrum of precipitation would result in better simulation of equatorial wave activity in the stratosphere**

Alexander *et al.* (2008) analyzed COSMIC GPS RO data and reported the global distribution of PE with vertical wavelengths ≤ 7 km

For comparison, calculated simulated PE ≤ 7 km

$$PE = \frac{1}{2}\left(\frac{g}{N}\right)^2 \overline{\left(\frac{T'}{\overline{T}}\right)^2}$$

Simulated PE ≤ 7 km consists of waves with

6 h < τ < 2 months, λz ≤ 7 km, ~380 < λx < 40000 km at the equator.

much wider spectral ranges in the AGCM data than COSMIC GPS RO

westerly shear (Uz>0) easterly shear (Uz<0)

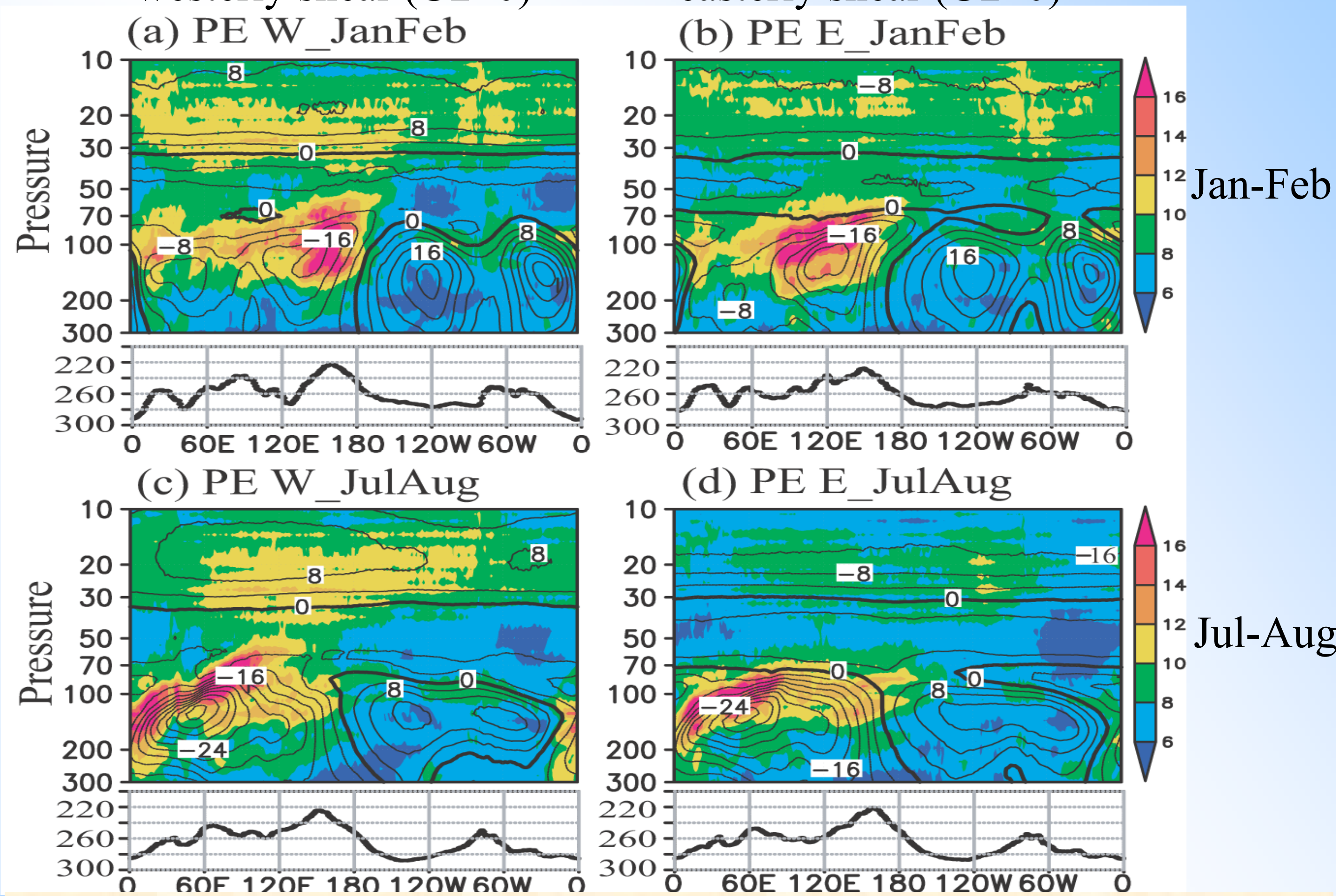

Fig.4: Lon-height cross-section of PE ≤ 7 km and zonal wind (10S-10N) (a, c) Westerly and (b, d) easterly shear phases of the QBO in (a, b) Jan-Feb and (c, d) Jul-Aug. Line graph indicates 2-monthly mean OLR

- Large convective activity in the EH and at ~60-80W
  In the UTLS, larger PE in the EH than in the WH
  →consistent with COSMIC.
- Larger PE is also distributed around the altitude where the zonal wind changes from easterly to westerly at approximately 30 hPa (Fig. a, c)
- Simulated PE ≤ 7 km > PE calculated using the COSMIC resulting from the much wider spectral ranges covered in the AGCM

Which phase velocities of waves contribute to PE ≤7km

eastern hemisphere (EH) | 10S-10N | western hemisphere (WH)

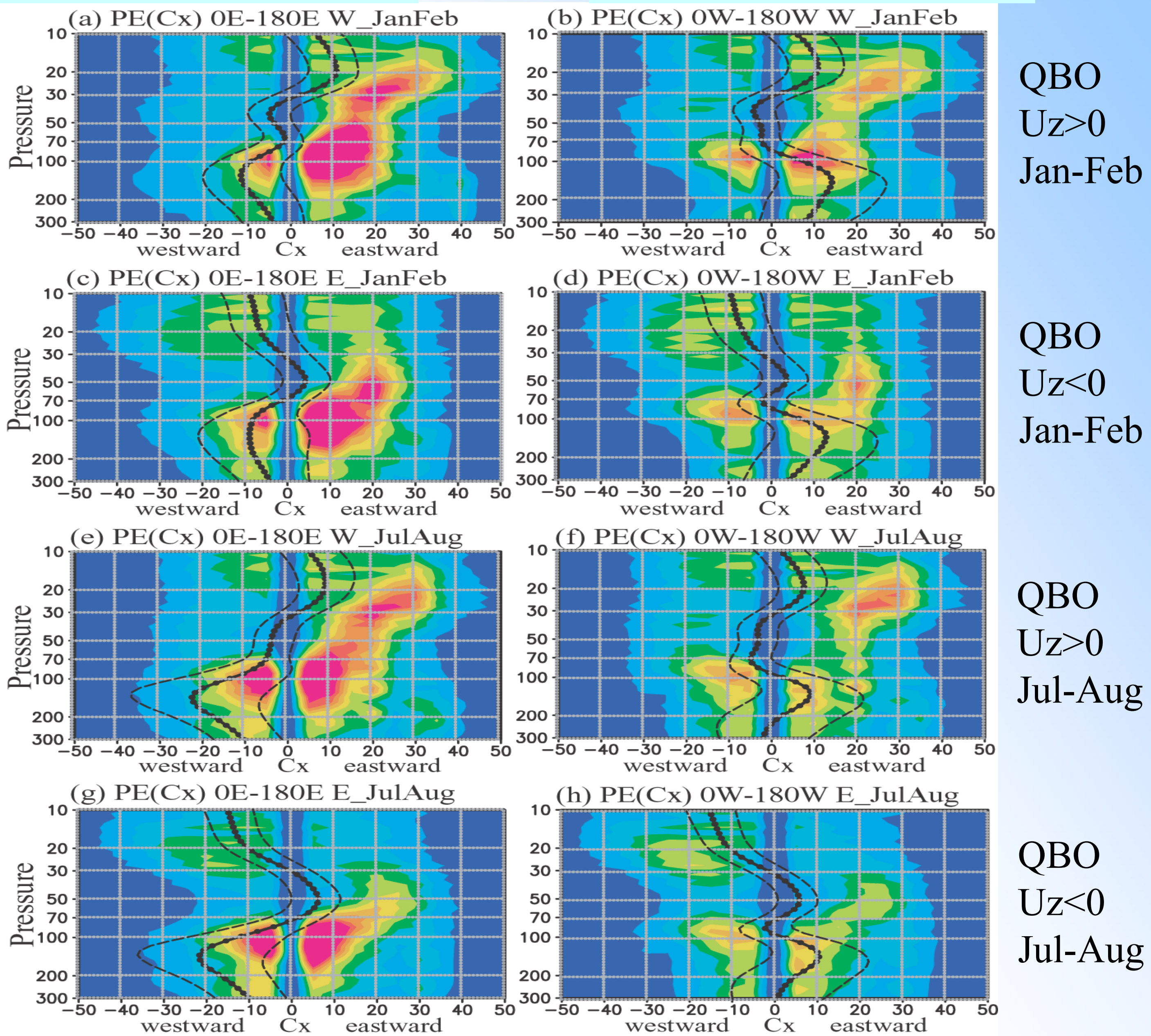

Fig.5: Height distributions of PE≤7 km as a function of Cx in the EH and WH. Vertical profiles of zonal wind $\lambda z > 7$ km ±standard deviation

- **In the EH**, easterly (westward wind) with the **Walker circulation allows most of eastward waves** to propagate from upper troposphere to the stratosphere, whereas **most of westward waves prevented** from entering stratosphere. **The situation is reversed in the WH**
- Wave sources are generally larger in the EH than WH in the UTLS
- In the stratosphere, waves are much influenced by the phase of QBO
  In Uz>0 in the EH (Fig.a,e), Cx changes ~10 ms^{-1} to 20 ms^{-1} at ~30hPa
  In Uz<0 PE with Cx~-10 ms^{-1} > PE with Cx~10 ms^{-1} (Fig.c,d,g,h)

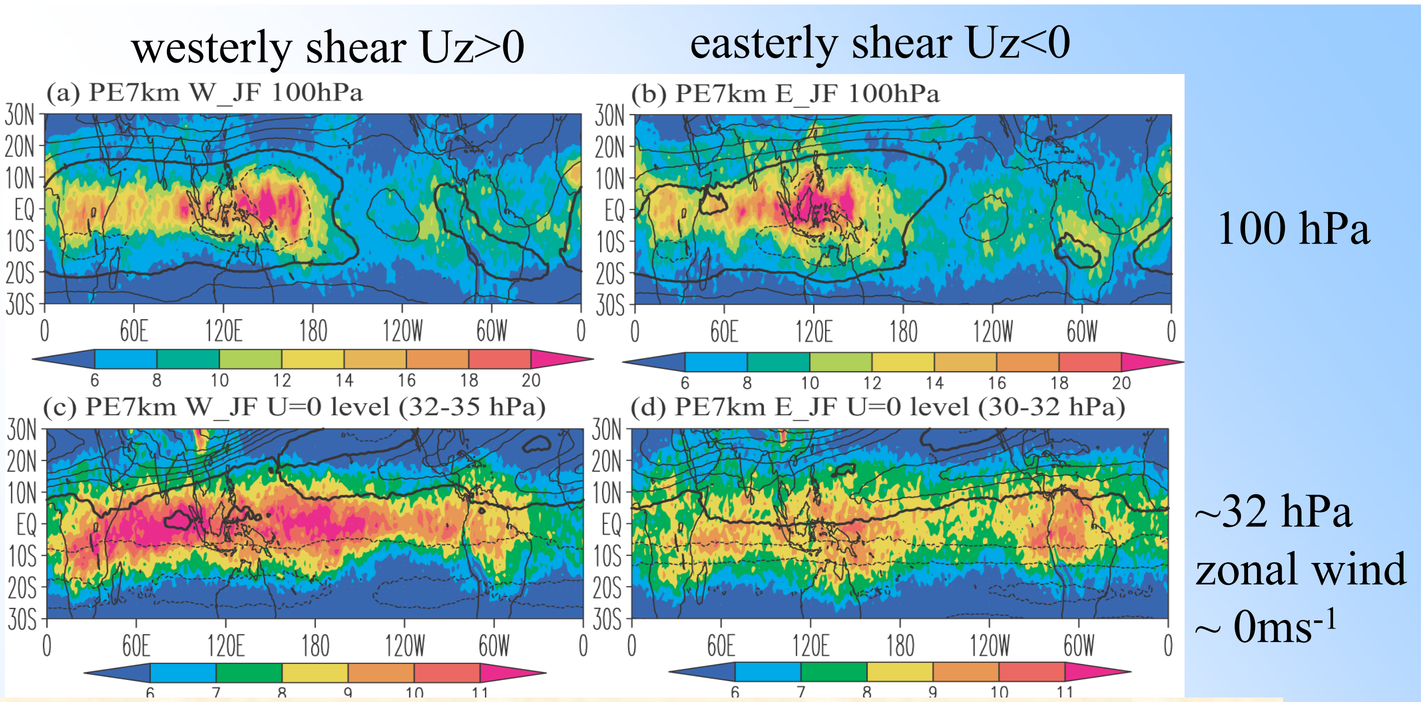

Fig.6: PE ≤7km at 100hPa & ~32hPa where U~0 m s^{-1} in Jan-Feb

- Little difference at 100 hPa between the two phases
- **Zonally elongating PE with larger** values above the equator in Uz>0
  Relatively **small PE with more scattered** distribution in the Uz<0
- Large PE is observed over South America in both Uz>0 and Uz<0.

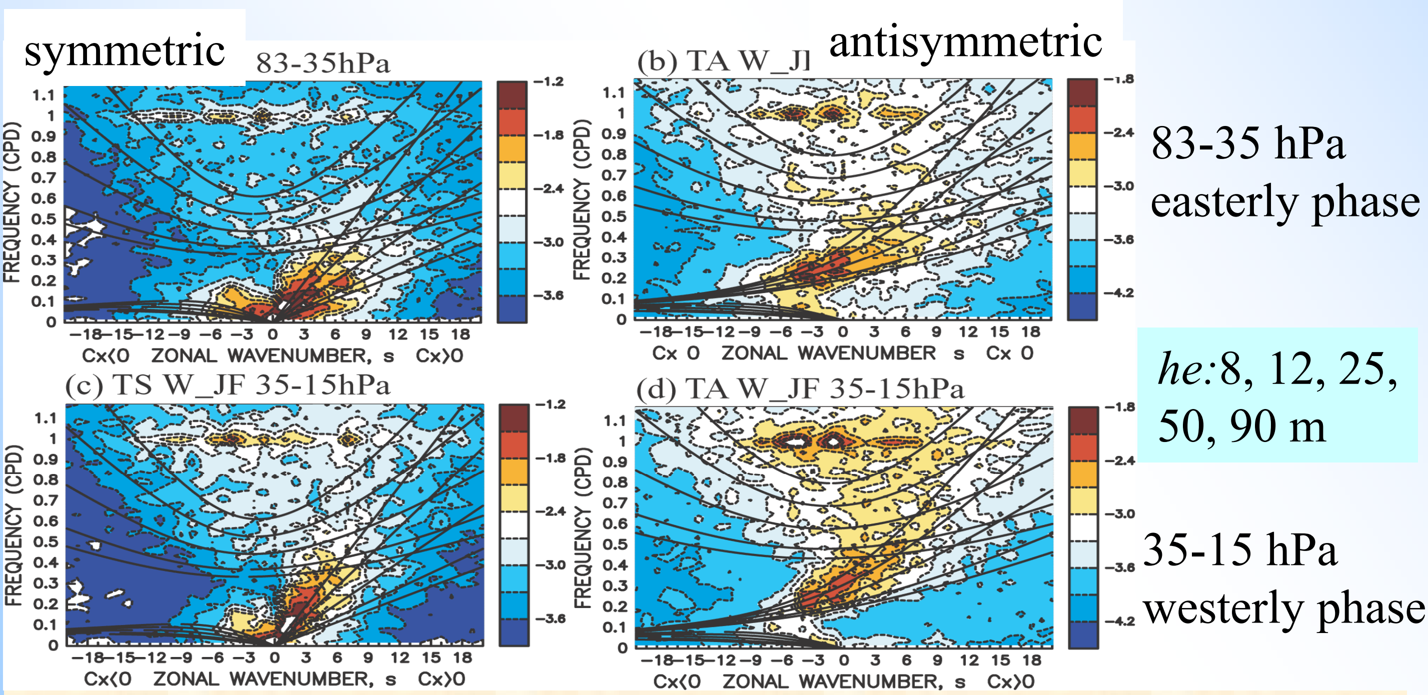

Fig.7: zonal wavenumber *vs.* frequency spectra of symmetric & antisymmetric of temperature for Uz>0 of QBO in Jan-Feb (10S-10N)

- Kelvin waves, MRG waves, n = 0 EIGWs, n = 1 ER in 8 ≤ he ≤ 90 m.
  connection of stratospheric EQWs & convectively coupled EQWs
- Kelvin and n = 0 EIGWs with he ~ 8 m decreased with height
- Other spectral peaks with periods of approximately 1 day

$\hat{\omega} = \omega - k\bar{u}$ $\hat{\omega}$:intrinsic frequency, ω:ground based frequency

- Ground-based frequency ω of a wave is defined at wave source level
- **ω and k do not change with altitude**, assuming a slowly varying background wind field, even if background wind changes with altitude.
- Distribution of k *vs.* ω spectra is independent of altitude; **distribution of the spectra would be changed only if a wave critical level filtering and/or wave dissipation occurs** (Ern et al. 2008).

To investigate the global distribution, sources and propagation of EQWs, an equatorial wave filter was constructed

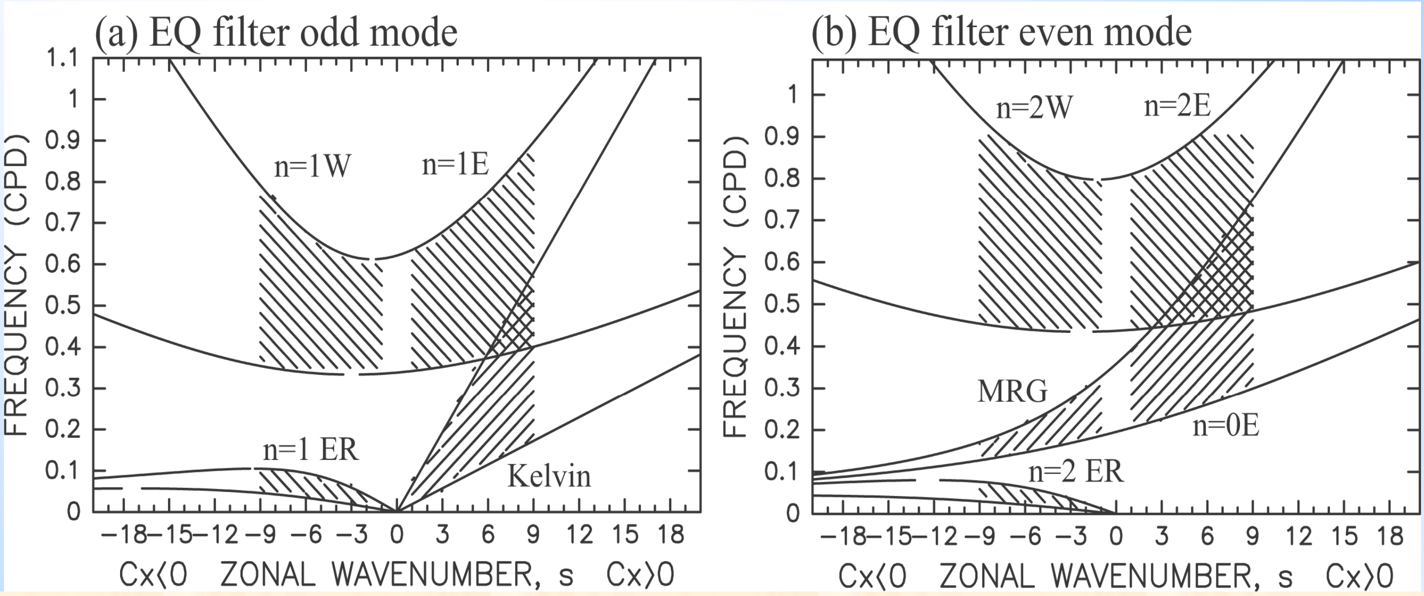

Fig.8: Equatorial wave filter for (a) odd and (b) even modes. Superposed are the dispersion curves of each EQW for two *he* of 8 and 90 m. Hatched areas between the two lines are the filtering range.

<Criteria>

- n= -1 (Kelvin wave) to n =2 mode
- **8<*he*<90 m** (~**2.3 km< λ z<~7.6km** for N^2 = 6 E-4 s^{-2})
- **1<*k*<9** (**4444km< λ x<40000km**), same as Alexander et al. (2008)
- minimum period: 1.1day to avoid including 1-day waves

- We describe application of the equatorial wave filter to unfiltered data (*i.e.*, original data with no temporal or spatial filtering)
- **The propagation properties of EQWs in relation to background winds from troposphere to stratosphere could be investigated using this filter, since ground-based frequency ω and zonal wavenumber *k* of a wave does not change unless a wave is dissipated**

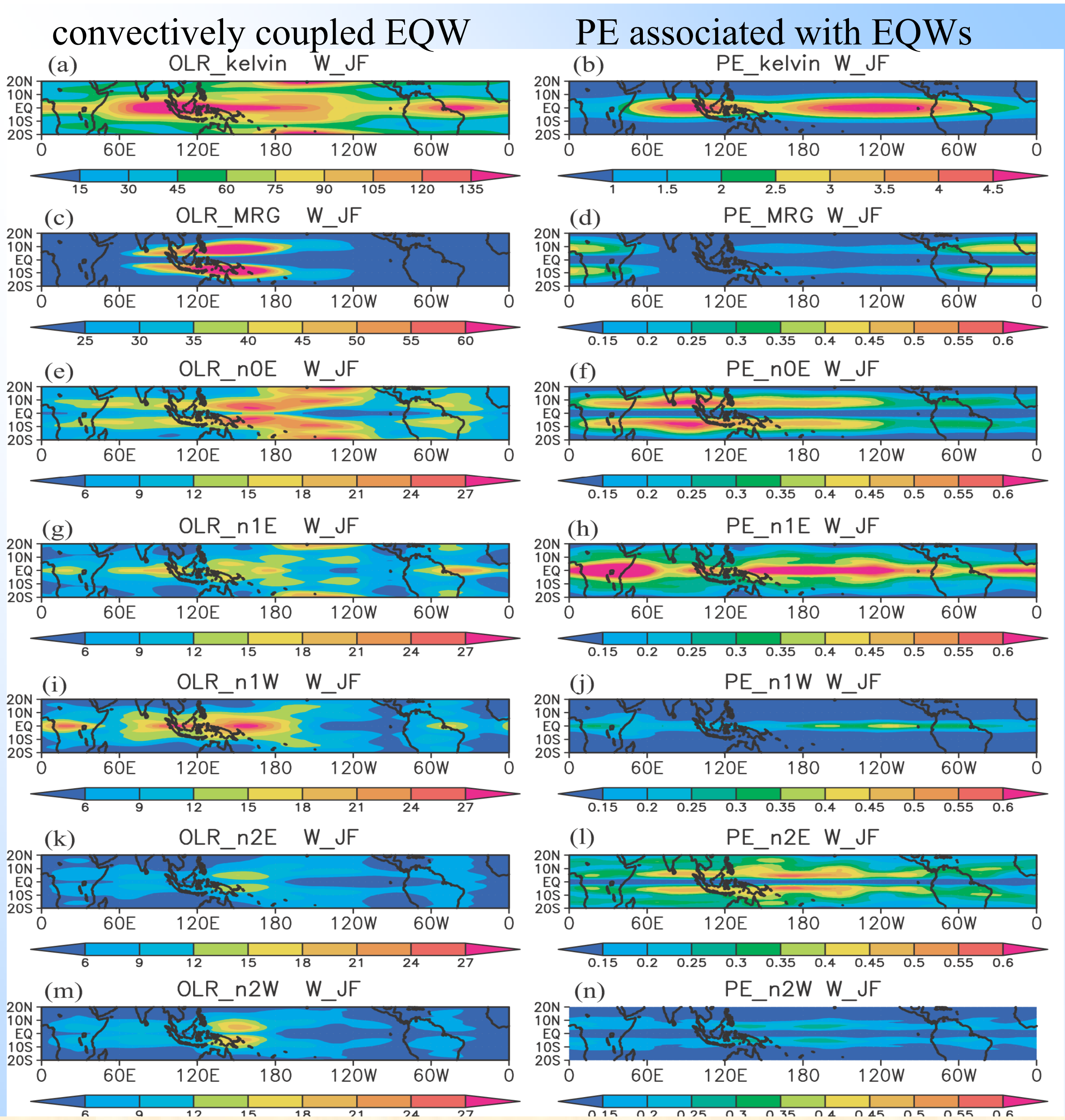

Fig.9: Global distribution of OLR variance due to convectively coupled EQW and PE due to EQW at 32-35 hPa in Jan-Feb during Uz>0 of QBO

- Distributions of simulated OLR variances are similar to those shown by Wheeler and Kiladis (1999) and Wheeler et al. (2000)
- For Kelvin waves, large PE located to the east of source distributions, suggesting eastward propagation of Kelvin waves from source region
- larger PE of n = 0 EIGW occurs over the Indian Ocean despite larger variance in OLR (Fig. 9e) in the Pacific than in the Indian Ocean
- Distributions of large PE with MRG and other EQWs **do not correspond directly** with those of the large variance in OLR.

Sources and propagation of equatorial trapped waves in Uz>0 of QBO

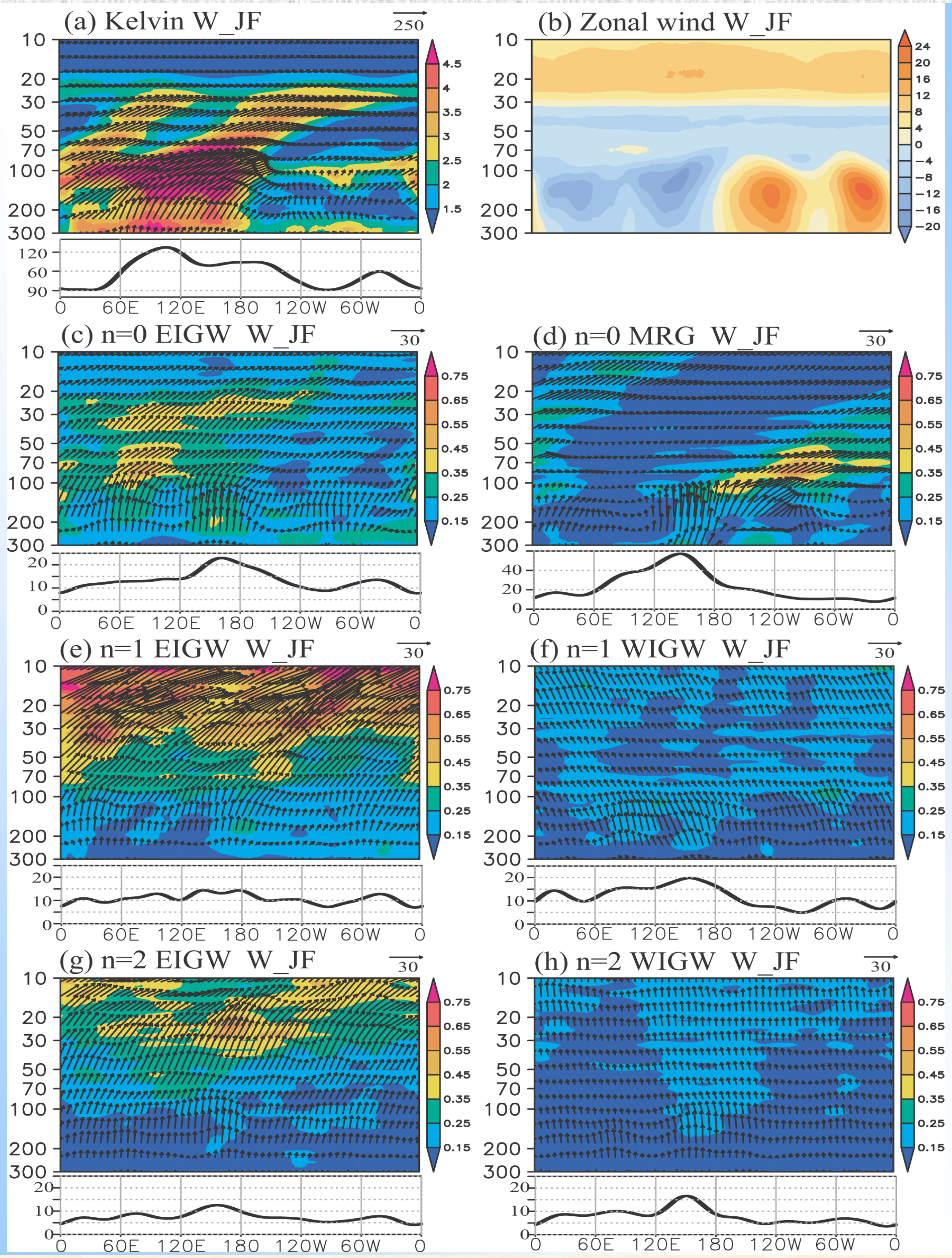

Fig.10: Longitude-height cross-sections of PE and horizontal and vertical energy fluxes due to each EQW in westerly shear in Jan-Feb (10N-10S) line graph indicates zonal variation in OLR variance due to each EWQ

Sources and propagation of equatorial trapped waves in Uz<0 of QBO

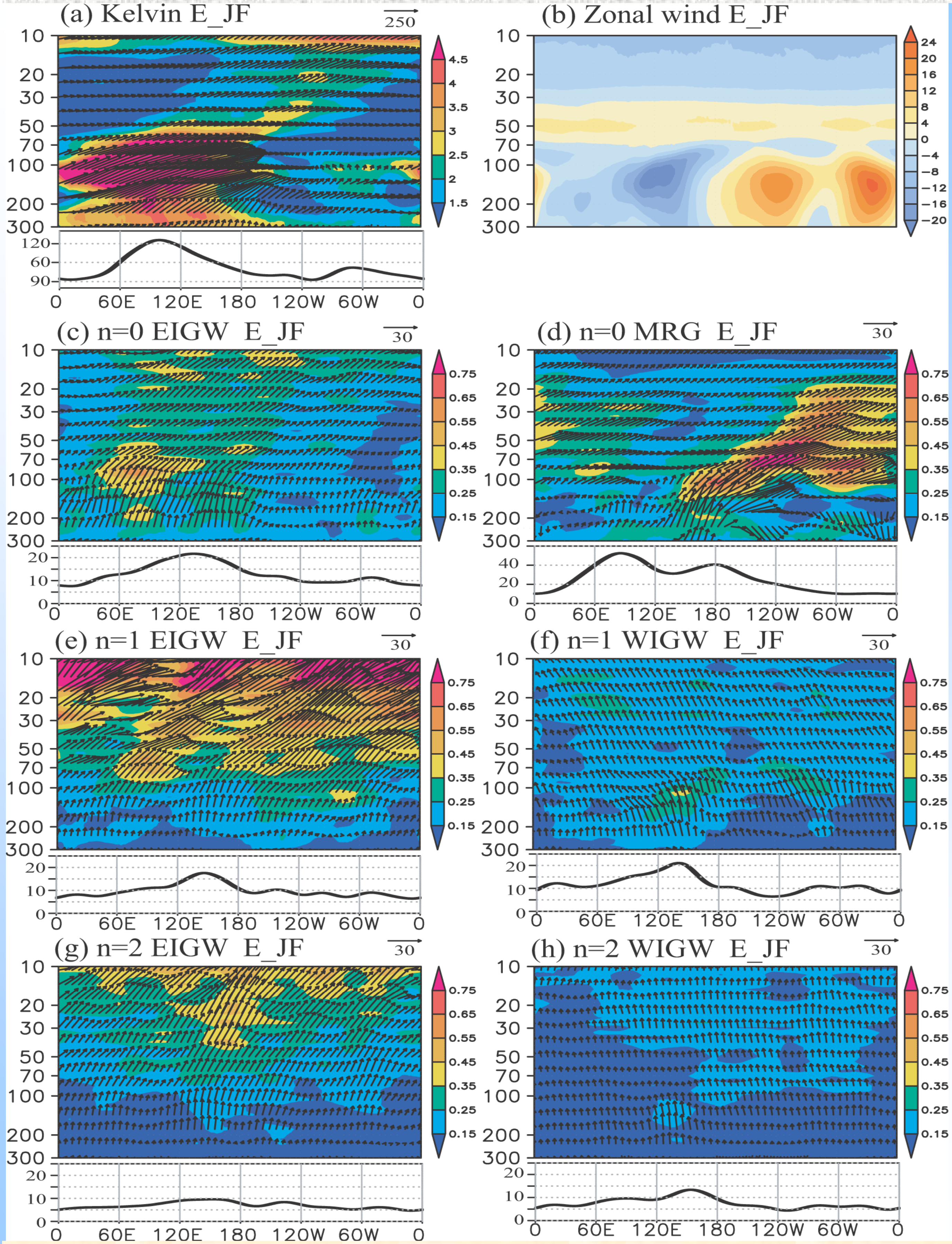

Fig.11: The same as Fig. 10, but for the easterly shear phase in Jan-Feb

To investigate the propagation of EQWs, energy fluxes are used.
The ratio of energy flux to energy density is equivalent to the ratio of wave action flux to wave action density in the case when the WKB theory is made in space and time. **The direction of wave group propagation is expressed by energy flux *F* to energy density *E*** as follows (Gill 1982):

$$\mathbf{F} = (\overline{\phi' u'}, \overline{\phi' w'}) = E(\hat{C}gx, \hat{C}gz),\ \ where\, E = 1/2(\overline{u'^2} + \overline{v'^2} + \overline{w'^2}) + 1/2(g/N)^2 \overline{(T'/\overline{T})^2}$$

- PE with Kelvin waves is most dominant among EQWs
- **Kelvin waves in EH with large sources propagate to stratosphere**
  Kelvin waves **in the WH become weak below 100 hPa** due to the westerly (eastward wind) associated with Walker circulation
- Energy flux decreases rapidly in the zonal direction around 180E
  Kelvin waves also dissipate also *via* horizontal propagation.

- In Uz>0, Kelvin waves become much weak at 20-30 hPa (Fig. 10a)
  In Uz<0, most Kelvin waves stop propagating at ~50 hPa (Fig. 11a)
  →**result in different global distributions of PE at ~32 hPa (Fig. 6c, d)**

- PE due to **MRG waves is large in the WH in the UTLS** region.
  Most MRG waves generated in the EH **do not enter the stratosphere, despite the large sources** (Figs. 10d & 11d), because the easterly with Walker circulation filters most of MRG waves in the upper troposphere
- MRG waves generated at approximately 150E-150W propagate eastward and upward and contribute to the PE in the stratosphere
- MRG wave propagate into the middle stratosphere (up to ~15 hPa) during Uz<0 of the QBO (Fig. 11d).

- In Uz>0, most of n = 0 EIGWs propagate until 20-30 hPa (Fig. 10c), where the zonal wind is 0-8 m s-1, and generate large PE at this altitude.
- At 70-30 hPa, more n = 1 WIGW propagate into middle stratosphere in Uz<0 (Fig. 11f) than Uz>0 of the QBO (Fig. 10f) as in MRG waves.
- In general, n = 1 and n = 2 EIGWs/WIGWs are not influenced much by the background zonal wind due to larger Cx

Distributions of stratospheric PE due to EQWs are greatly affected by source distribution, the Walker circulation, and the QBO phase.
Stratospheric variation (interannual and seasonal variation) of PE should be associated with tropospheric variation in addition to QBO

The ratio between equatorial trapped waves and 3-D gravity waves

Which EQWs and/or 3D-gravity waves contribute to the PE ≤ 7 km

To assess this question, equatorial wave filter was used for T’ ≤ 7 km.

westerly shear phase Uz>0 | easterly shear phase Uz<0

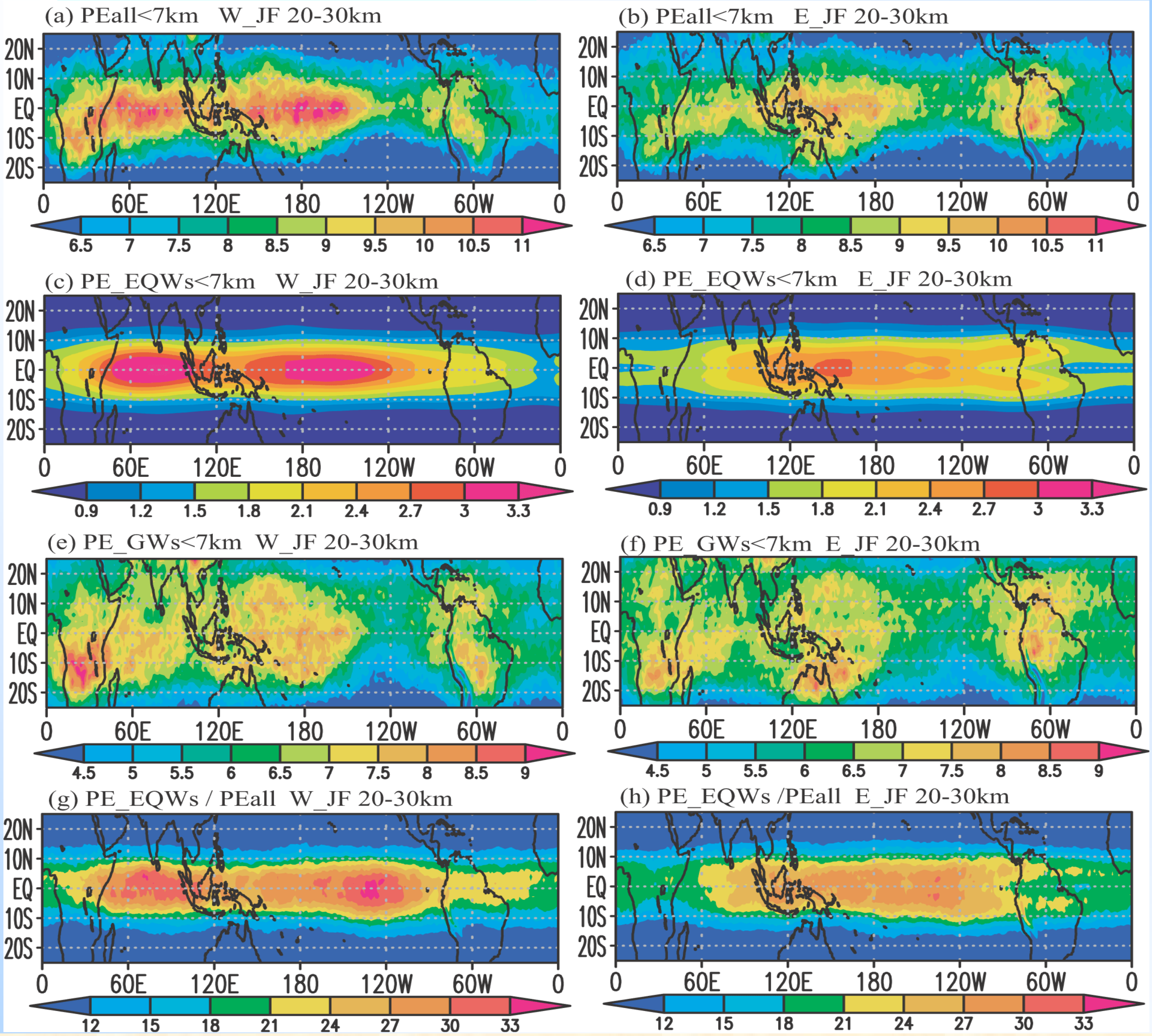

Fig.12: (a, b) Global distribution of total PE ≤7 km at 20-30 km
PE due to (c, d) EQW ≤7 km and (e, f) 3D-gravity wave ≤7 km.
(g, h) ratio between total PE≤7km and PE due to EQWs≤7 km in Jan-Feb

- **PE ≤ 7 km in the Uz>0 is generally larger than that in the Uz<0**
- In Uz>0 PE with EQWs is larger with dominant symmetric structures
- In Uz<0, off-equatorial structures of PE with EQWs were clearly seen
- PE with 3D-gravity waves shows a scattered structure.
  Large over Congo basin, South America, the Indian Ocean etc.
- **Up to ~30% is contributed by EQWs, 3D-gravity waves ~70%**
- The contribution of EQWs to PE is smaller over the Atlantic Ocean.

Gravity waves with period ≤ 24 hours

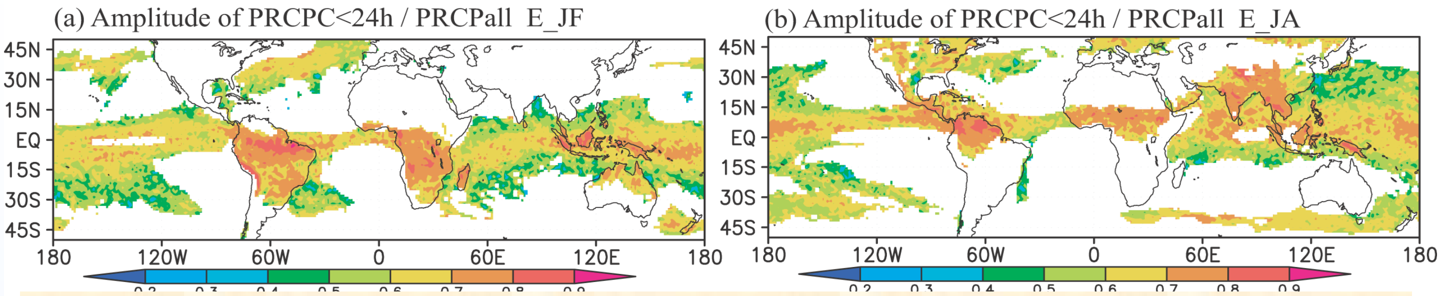

Fig. 13: Amplitude of cumulus convection with periods ≤ 24 h for (a) Jan-Feb and (b) Jul-Aug during the easterly phase (Uz<0) of QBO
→similar to observation (Ricciardulli and Sardeshmukh 2002)

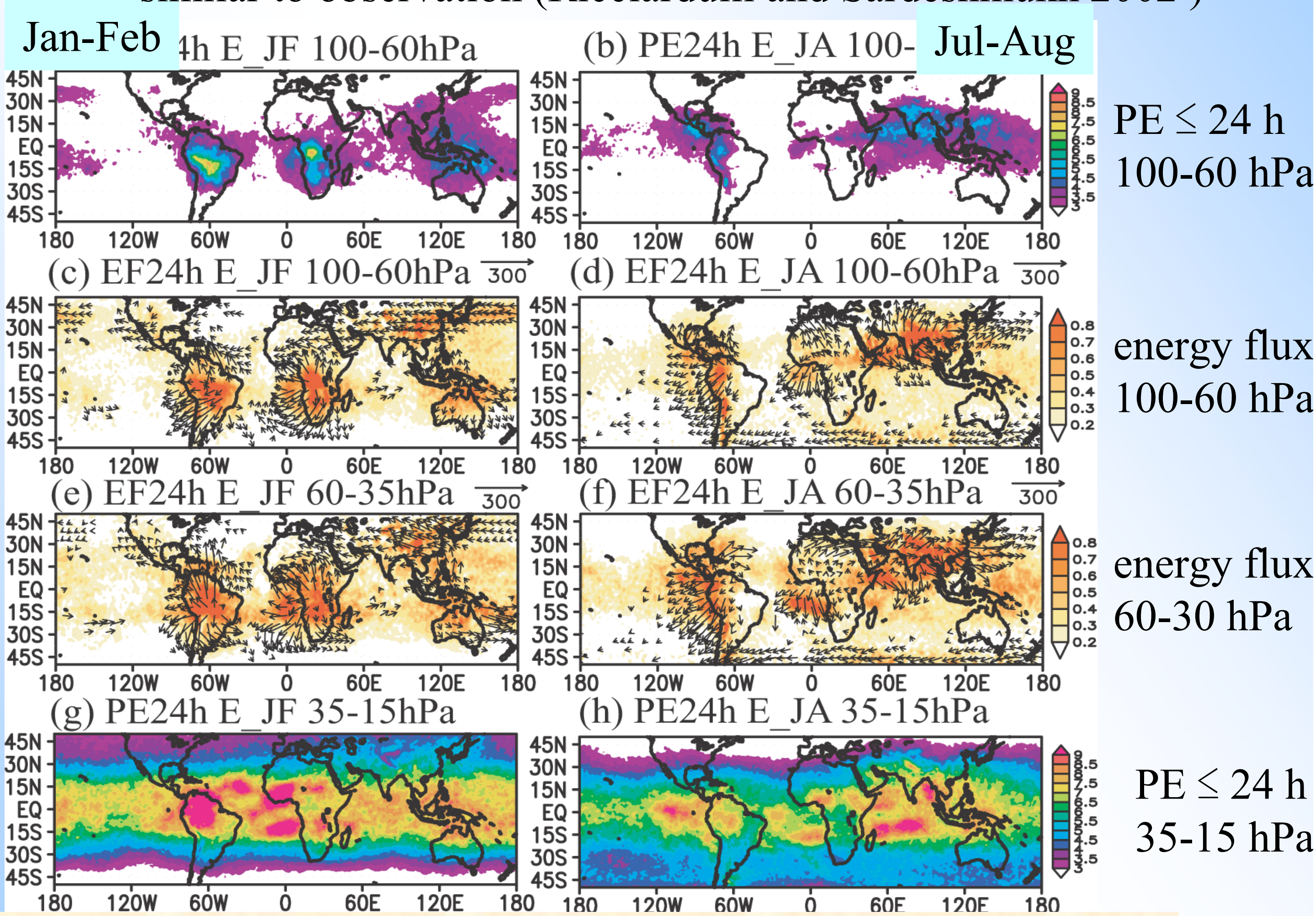

Fig. 14: PE and energy flux≤24 h during Uz<0 of the QBO
(c-f) vertical energy fluxes greater than 0.2 J $kg^{-1}m\ s^{-1}$ are shaded

- In Jan-Feb, localized PE over South America, Congo Basin around Indonesia at 100-60 hPa; In Jul-Aug, over South America to Guatemala and over the Bay of Guinea and the Indian monsoon region.

→**correspond well to distribution of much precipitation≤24 h**

- 3D-gravity waves generated in these areas propagate 3-dimensionally large PE to stratosphere in areas a short distance from the source region

Summary

- Global distribution, sources, and propagation of EQWs and 3D-gravity were investigated in the AGCM with T106L60 resolution.
- zonal wavenumber *vs.* the frequency spectra of precipitation represents realistic signals of convectively coupled EQWs.
- Each EQW in the stratosphere generally corresponded well with source of each convectively coupled EQW activity in the troposphere.
- The propagation of Kelvin waves, MRG waves, and n = 0 EIGWs is strongly influenced by the Walker circulation and the phase of the QBO.
- Similar characteristics between COSMIC GPS RO data and the AGCM
  (1) Much larger PE elongates over EH than in the WH in UTLS region
  (2) In the middle stratosphere, zonally non-uniform PE distributions are more apparent in $Uz<0$ than $Uz>0$ of the QBO.
  (3) Stratospheric Kelvin wave generally larger in the EH than the WH
  (4) Dominant MRG in the westerly than the easterly phase of QBO
- The different vertical shear of the Walker circulation between the EH and WH plays an important role in wave filtering, which results in different PE distributions between EH and WH in the UTLS region.
- Distributions of stratospheric PE associated with EQWs are affected by (1) source distribution, (2) the Walker circulation, and (3) the QBO phase
- EQWs≤7km contribute up to ~30% of total PE≤7 km in the stratosphere
  →3D-gravity waves ≤ 7 km account for ~70% of the PE ≤ 7 km
- 3D-gravity waves generated over strong precipitation ≤24 h contribute to localized PE ≤ 24 h at short distances from the source region.
- The global distribution of PE depends on the height, background wind (the QBO and Walker circulation), and wave sources. In the real atmosphere, PE in the stratosphere should show distinct interannual and seasonal variation, associated with tropospheric variability .
- analysis with longer period and more accurate simulation is needed

Lon-Time Kelvin and MRG wave at 22 km

COSMIC Results during 2007

Kelvin 8<he<90

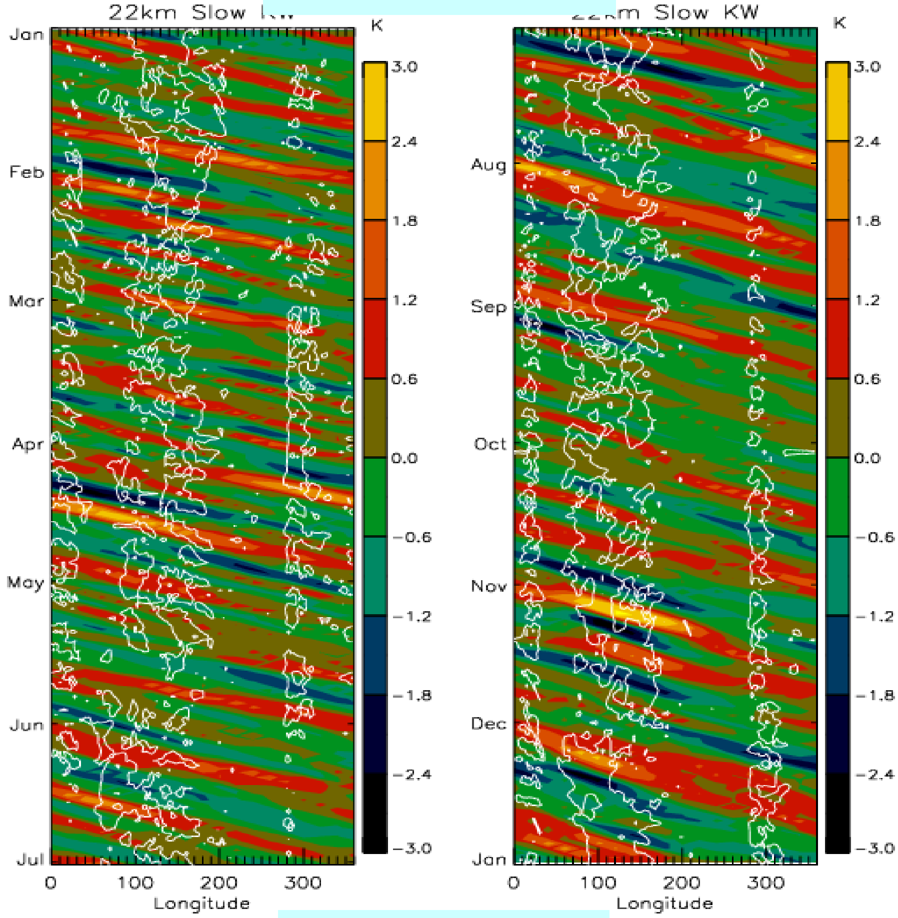

- Mostly $k = 1, 2$
  T’ up to 2 – 3K,
  periods ~ 10-20 days
  Cx ~ 15 – 30 m s-1.
- amplitude EH > WH
- $k = 3, 4$ waves with shorter periods, smaller amplitudes $Cx \sim 20 - 30$ m s^{-1} (e.g. early Jan, early May, late Sep.)

MRG 8<he<90

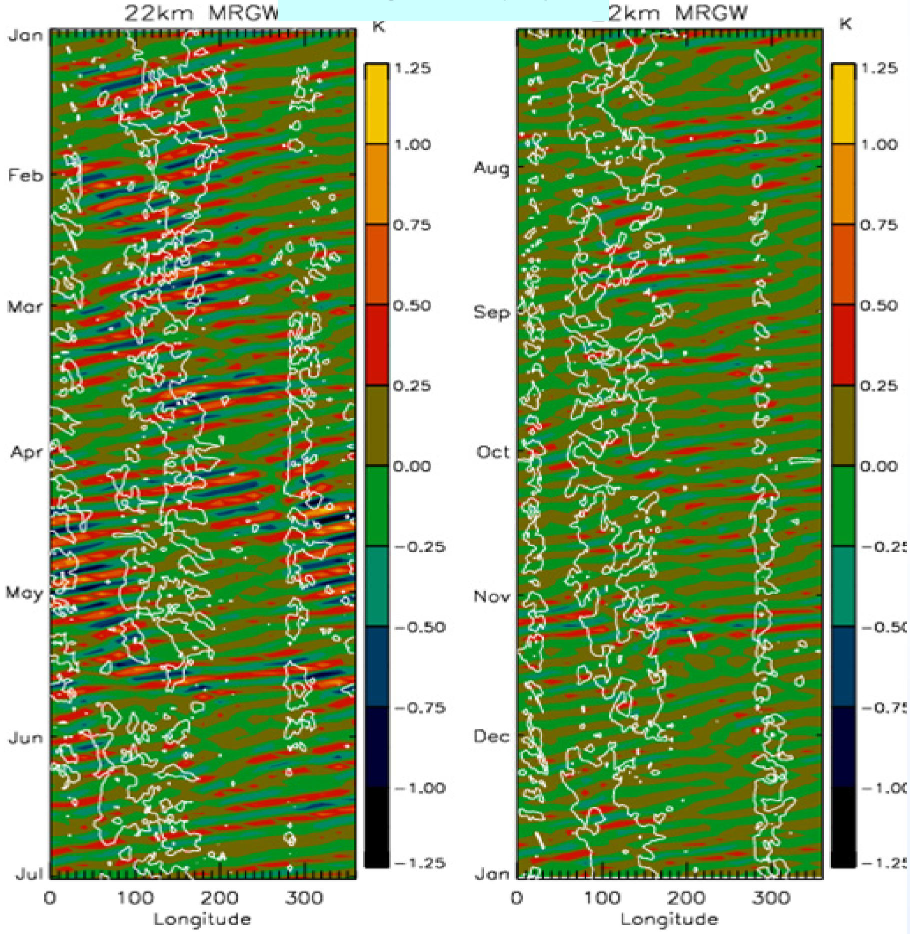

- packet eastward Cgx>0
- waves westward Cx<0
- Sudden decrease after May when the QBO phase becomes easterly
- Periods 3 – 5 days, T’ up to ~1.2K, $Cx \sim 20 - 30$ m s^{-1}, $k > -5$

Monthly temperature variance of MRG waves COSMIC during 2007

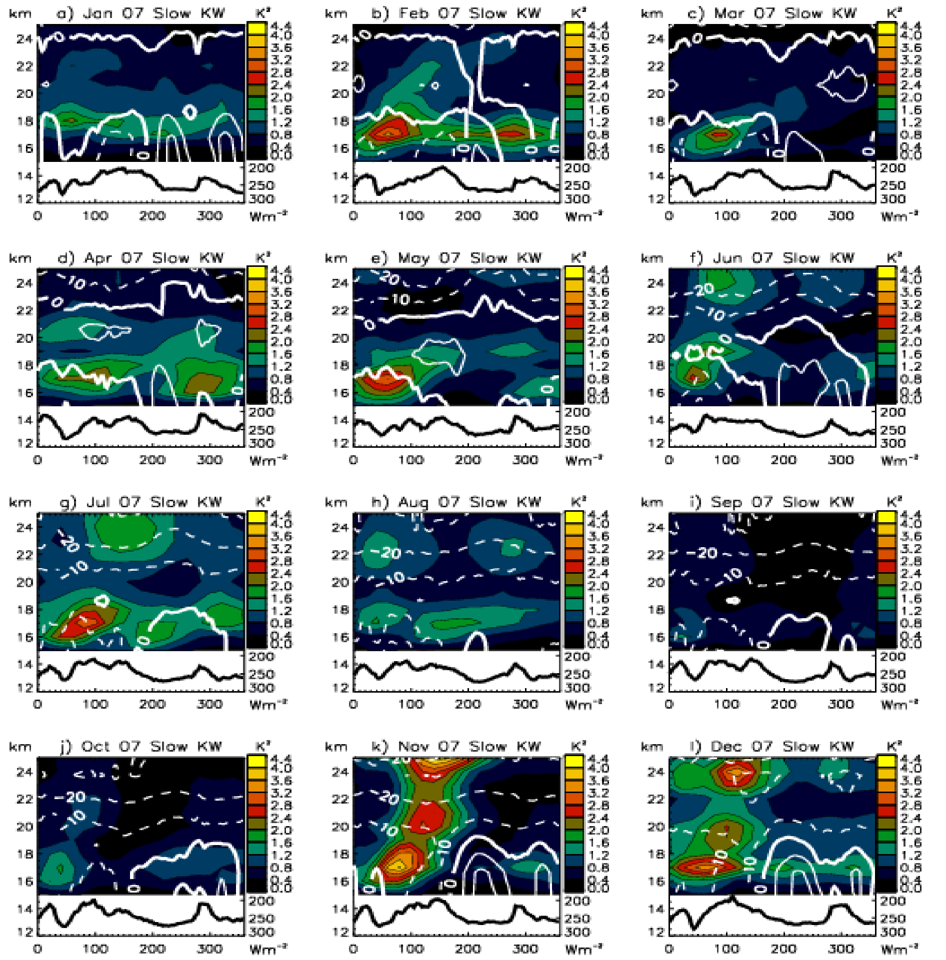

<Kelvin wave>

- significant monthly variability in UTLS
- eastward & upward propagation
- more propagation from the troposphere to the stratosphere in easterly phase of the QBO
- large activity in EH than in WH

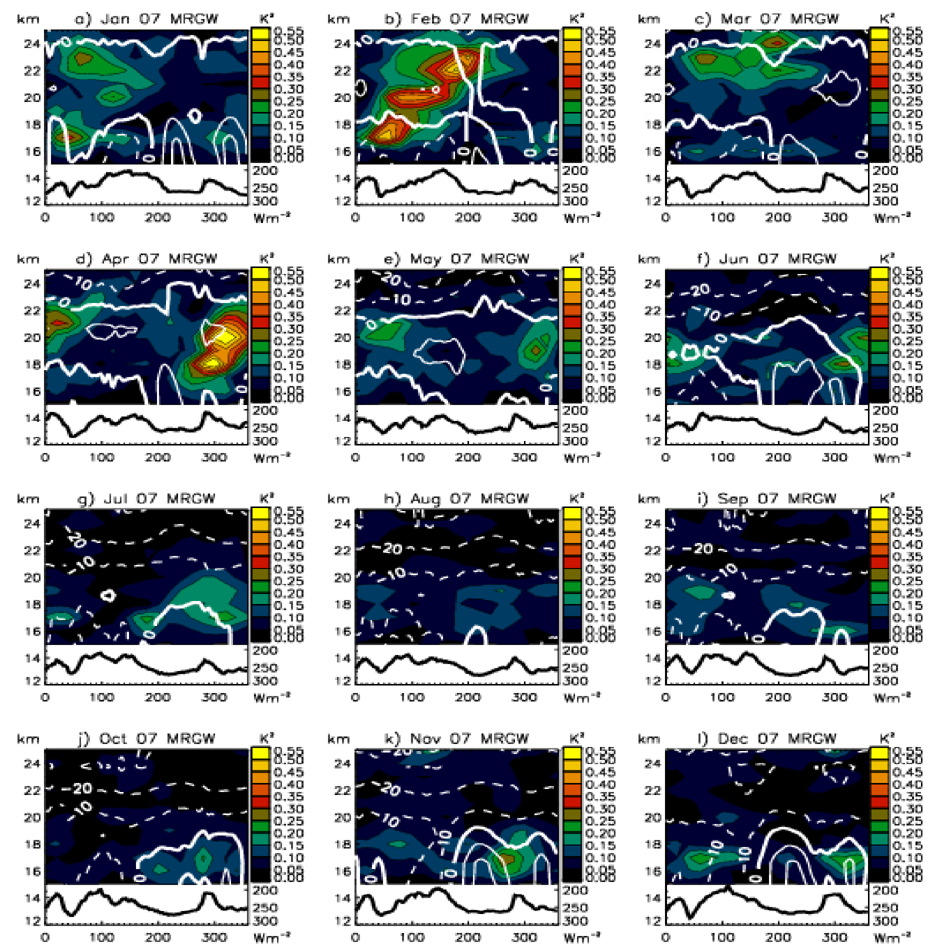

<MRG wave>

- Large variance in the stratosphere during the westerly phase of QBO
- Small variance after May when phase of QBO become easterly
- In the UTLS region, more MRG wave in the WH in Sep-Dec